involved. The first diagram shows the processes used in the present work. The second diagram shows schematics for the DFWM and LIF processes. These two techniques involve the same molecular transition (and thus the same molecular quantum-state population density), but each of these processes has a different functional dependence on the molecular quantum-state quenching rate, $Q$ (*14*). This difference can be exploited to solve for $Q$, and by so doing, the need to measure $Q$ separately and for each molecular collision partner can be avoided. This multiplex experiment would enable LIF, a very sensitive spectroscopic technique, to determine absolute concentrations of molecular species. The third diagram shows schematics for Raman and CARS spectroscopies. Raman and CARS involve the same two-photon molecular transition, but each of these processes has a different functional dependence on the molecular transition linewidth, $\Gamma_{rg}$ (*15, 16*). The two formulas that describe Raman and CARS spectroscopic signal generation can be used as simultaneous equations to determine $\Gamma_{rg}$, even if the linewidth of the probe laser greatly exceeds the linewidth of the spectroscopic transition. As a final example, we show two diagrams for DFWM spectroscopy. This technique can be implemented as a diagnostic probe in either the high or low optical power limits (*3, 4*). The fact that the DFWM signal generated in each of these power limits has a different functional dependence on $\mu_{21}$ indicates that DFWM can be used to find $\mu_{21}$ and $\Delta N$, if this aspect of the technique is exploited. Clearly, numerous unexplored opportunities exist to exploit current spectroscopies in new ways to make hitherto unattainable measurements.

## REFERENCES AND NOTES


1. H. Walther, *Laser Spectroscopy of Atoms and Molecules*, H. Walther, Ed. (Springer-Verlag, Heidelberg, 1976).
2. W. Demtröder, *Laser Spectroscopy Basic Concepts and Instrumentation* (Springer-Verlag, Heidelberg, 2nd printing, 1982).
3. P. H. Vaccaro, *Adv. Phys. Chem.*, in press.
4. R. L. Farrow and D. J. Rakestraw, *J. Opt. Soc. Am. B* **9**, 1770 (1992).
5. G. J. Germann, A. McIlroy, T. Dreier, R. L. Farrow, D. J. Rakestraw, *Ber. Bunsenges. Phys. Chem.* **97**, 1630 (1993).
6. G. J. Germann and D. J. Rakestraw, unpublished results.
7. The absorption spectrum is taken as the ratio of the transmitted laser power to the input laser power to correct for shot-to-shot laser-power fluctuations.
8. The $b_p$ value of 0.074 ± 0.004 $cm^{-1}$/atm was used for the (101)-(000) vibrational band of $NO_2$. This value was obtained from the average of the $b_p$ values for the (010)-(000) and (001)-(000) vibrational bands of $NO_2$, 0.071 ± 0.004 [R. D. May and C. R. Webster, *Geophys. Res. Lett.* **17**, 2157 (1990)] and 0.077 ± 0.006 $cm^{-1}$/atm [V. M. Devi *et al.*, *J. Mol. Spectros.* **84**, 234 (1980)], respectively.
9. R. L. Abrams, J. F. Lam, R. C. Lind, D. G. Steel, P. F. Liao, in *Optical Phase Conjugation*, R. A. Fisher, Ed. (Academic Press, New York, 1983), p. 211.
10. R. L. Abrams and R. C. Lind, *Opt. Lett.* **2**, 94 (1978).
11. A. S. Pine and J. P. Looney, *J. Mol. Spectros.* **122**, 41 (1987).
12. R. A. Toth and R. H. Hunt, *ibid.* **79**, 182 (1980).
13. A. S. Pine, A. Fried, J. W. Elkins, *ibid.* **109**, 30 (1985).
14. P. M. Danehy, E. J. Friedman-Hill, R. P. Lucht, R. L. Farrow, *Appl. Phys. B* **57**, 243 (1993).
15. S. A. J. Druet and J.-P. E. Taran, *Prog. Quantum Electron.* **7**, 1 (1981).
16. A. C. Eckbreth, *Laser Diagnostics for Combustion Temperature and Species*, A. K. Gupta and D. G. Lilley, Eds. (Abacus Press, Cambridge, MA, 1988).


17. We thank R. L. Farrow for developing the spectral simulation software used to analyze the experimental data, G. A. Hux for technical support, and R. L. Farrow and P. H. Paul for useful discussions. Supported by the U.S. Department of Energy, Office of Basic Energy Sciences, Division of Chemical Sciences.

8 February 1994; accepted 9 May 1994


# Higher Order Self-Assembly of Vesicles by Site-Specific Binding


Shivkumar Chiruvolu, Scott Walker, Jacob Israelachvili, Franz-Josef Schmitt, Deborah Leckband, Joseph A. Zasadzinski*



**The association of lipid molecules into spherical vesicles in solution as a result of nonspecific intermolecular forces constitutes a primary self-assembly process. Such vesicles can undergo a secondary self-assembly into higher order structures in a controlled and reversible manner by means of site-specific ligand-receptor (biotin-streptavidin) coupling. Cryoelectron microscopy shows these structures to be composed of tethered, rather than adhering, vesicles in their original, unstressed state. In contrast, vesicles aggregated by nonspecific, such as van der Waals, forces are deformed and stressed, producing unstable structures. Vesicle association by site-specific binding provides a practical mechanism for the production of stable, yet controllable, microstructured biomaterials.**


Much of the recent interest in self-assembling structures, in which surfactant or polymeric molecules in solution spontaneously assemble into large, thermodynamically stable structures with well-defined geometries, springs from the close association of this process with living systems (*1–4*). The simplest and most studied of these biomimetic structures are unilamellar vesicles, which are single, spheroidal bilayer shells encapsulating an aqueous interior (*2–4*). Proteins and other biologically active molecules can be incorporated into the vesicle bilayer or interior, thereby serving as models of biological cells (*2–4*). Vesicles are also currently being developed for drug delivery applications (*3*). However, the analogy to living systems is, as yet, incomplete. There are invariably several levels of self-assembly in even the simplest cell or tissue. The next, or secondary, level of self-assembly is achieved through the specific, but reversible, association of vesicles into stable multivesicle aggregates by means of ligand-receptor coupling. Such structures should serve as idealized models for biological tissues, and their spontaneous formation in the laboratory could lead to new methods for processing artificial tissues and "soft" composite materials.

The self-assembly of molecules and small aggregates in solution into larger structures is brought about by a number of attractive forces: van der Waals, ion-binding, hydrophobic, polymer bridging, and depletion forces, as well as lock-and-key type interactions (*5*). Apart from the last, all of these forces may be considered nonspecific because they act indiscriminately between all parts of the particles. The resulting adhesion is usually described in terms of the adhesion energy, $W$, which is the reversible work done on bringing two surfaces of unit area into adhesive contact. By definition, $W = 2\gamma$, where $\gamma$ is the surface or interfacial energy per unit area (*5*).

When two soft colloidal particles or vesicles aggregate as a result of nonspecific forces, they deform elastically to increase their mutual area of contact as much as possible (similar to the mutual flattening of two adhering soap bubbles). Such vesicle deformations can be imaged by electron microscopy. For example, phosphatidylcholine (PC) vesicles can be induced to aggregate by stressing them osmotically (Fig. 1), which suppresses the repulsive undulation force and enhances the attractive hydrophobic force between them (*6, 7*). Similar deformed structures are produced by other types of nonspecific surface forces, for example, when negatively charged vesicles are aggregated by addition of calcium ions to the solution (*8, 9*). These deformations cause large elastic strains and stresses on bilayers and membranes, which result in


Department of Chemical Engineering, University of California, Santa Barbara, CA 93106, USA.

*To whom correspondence should be addressed.

increased fragility, leakage, lysis, and fusion (*10–13*). In general, the stronger the adhesion energy, the larger the deformations (*6–14*), and vesicle aggregation by colloidal-type surface forces is bound to be limiting for the design of robust, higher order self-assembly processes.

No such deformations and accompanying stresses and strains should occur when vesicles are brought together by a specific site-binding interaction. This is because the whole vesicle surface is not involved in the interaction, but only a discrete number of highly localized ligands and receptors on each surface. The resulting adhesion energy is therefore not expected to be dependent on the surface energy or vesicle size, but on the discrete strength and number of such bonds formed per vesicle.

To test this hypothesis, we prepared unilamellar vesicles by first mixing dilauroylphosphatidylcholine (DLPC) with dipalmitoylphosphatidylethanolamine-conjugated biotin (DPPE-biotin) in chloroform solution and then removing the solvent thoroughly under vacuum. The mixed lipids were hydrated in an aqueous 0.2 M NaCl and 0.2 mM phosphate buffer to form a multilamellar liposome dispersion. The dispersion was repeatedly frozen in liquid nitrogen and thawed, followed by repeated extrusions through stacked Nucleopore filters of specific pore size 100 nm, to form a monodisperse population of unilamellar vesicles (*15*). The resulting ligand-vesicle solution of overall concentration 30 mg/ml was clear and light blue in color and consisted of vesicles of mean radius 50 nm with about 80 DPPE-biotin ligands per vesicle exposed on the outer monolayer. In earlier studies, streptavidin (*16*) and various antibodies (*17*) retained their activities after they were specifically bound to vesicles. Also, receptor proteins can be isolated from a complex mixture by means of site-specific binding to biotinated vesicles (*18, 19*).

Adding sufficient streptavidin in the same buffer (1.34 mg/ml) to the ligand-vesicle solution (a ligand-receptor mole ratio of about 7:1) caused the vesicles to aggregate immediately. After a few minutes, the aggregates were sufficiently large to settle from the solution. Subsequent cryoelectron microscope imaging of the aggregates (*20*) (Fig. 2, A and B) showed that the vesicles had aggregated with only minimal changes in shape or size. This indicates that the vesicles remained unstressed during aggregation. Virtually all of the vesicles were present in the large aggregates; few free vesicles were seen in the micrographs. The aggregates were bound together strongly enough that they did not break up, even during the relatively large shears necessary to form thin samples for cryoelectron microscopy (*20*).

No such aggregates were seen in control experiments where (i) streptavidin was added to a solution of pure DLPC vesicles and (ii) streptavidin inactivated by soluble biotin was added to a ligand-vesicle solution (Fig. 3). The binding mechanism most consistent with all the data is one in which vesicles are tethered together by streptavidin (Fig. 2C).

Often, the aggregation of colloidal particles brought about by nonspecific forces can be reversed. For example, calcium-induced adhesion can be reversed if a chelating agent is added (*8, 9*). However, one of the benefits of the ligand-receptor bond is its strength, so our initial thought was that binding would be irreversible and thus difficult to control. This would present a serious limitation to any site-binding aggregation process of any complexity. Fortunately, ligand-receptor bonds can be reversed by the addition of an even higher affinity analog agent to the solution; that is, one that competes effectively with, and eventually replaces, the original bound ligand.

To demonstrate reversibility, we added soluble biotin to the solution of aggregated vesicles at a 10-fold excess of soluble biotin to streptavidin. Soluble biotin has a significantly higher binding affinity for streptavidin than DPPE-biotin (*18, 21*). After 30 min of incubation, the vesicles had spontaneously redispersed back to their original state (Fig. 3A); the solution was again clear and bluish, and in cryoelectron micrographs, the vesicles appeared almost identical in size and shape to their appearance before aggregation.

A second series of experiments, procedurally identical to the above, was conducted with vesicles of DLPC mixed with *N,N*-dioctadecylamide–desthiobiotin (DODA-desthiobiotin), a biotinated lipid analog (*22*) whose binding constant with streptavidin is estimated to be about two orders of magnitude smaller than that of DPPE-biotin (*21*). The results were qualitatively very similar; the main difference is that when

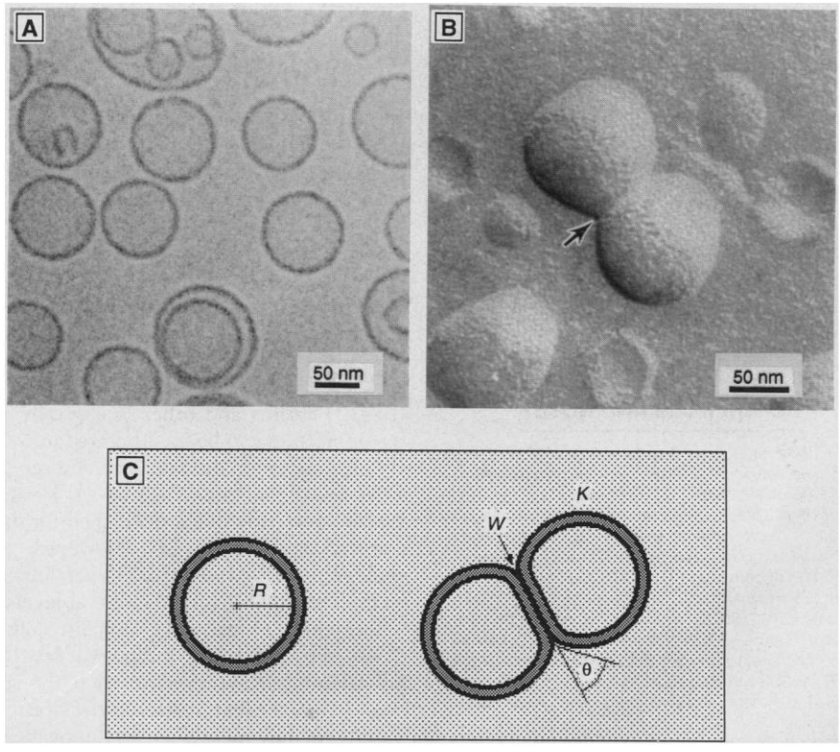


**Fig. 1.** (**A**) Cryoelectron micrograph of unstressed, spherical PC vesicles in aqueous solution. Specimens were prepared for imaging by the method of Bellare *et al.* (*20*). The sample shown here contained 100 mg of PC per milliliter of pure water, which was rapidly frozen (at >15,000 K $s^{-1}$) from a temperature of 38°C. All lipids were from Avanti (Alabaster, Alabama). (**B**) Freeze-fracture electron micrograph of similarly prepared vesicles in adhesive contact after they were made to aggregate by increased hydrophobic interactions caused by osmotic stress. The vesicles were osmotically swollen before freezing by a 10 mM glucose concentration difference between the inside and outside of the vesicle; this exposes more of the hydrophobic hydrocarbon chains of the bilayer to the aqueous phase, which increases the adhesion energy from $W \approx 0.01$ to 0.1 mJ $m^{-2}$ (*6, 7*). (**C**) Schematic geometry of nonadhering and adhering vesicles in solution corresponding to the images shown in (A) and (B). *R*, radius; *W*, adhesion energy; *K*, elastic area expansion modulus; and θ, angle of contact.

soluble biotin was added to the aggregated vesicle solution, the redispersion occurred much more quickly, taking a few minutes rather than ~30 min. The faster redispersion is consistent with the lower binding constant of streptavidin with desthiobiotin as compared with DPPE-biotin.

The above results are consistent with a simple theoretical treatment of vesicle aggregation as well as with previous measurements of biotin-avidin and biotin-streptavidin bond strengths. When two initially unstressed spherical vesicles of radius $R$ adhere, the attractive adhesion force pulls the two membranes together so that they deform elastically (Fig. 1C). A convenient measure of this deformation is the contact angle, $\theta$, subtended by the surfaces just outside the flattened contact zone (Fig. 1). If the vesicles initially deform at constant internal volume (assuming negligible water permeation, which should be the case on initial contact), the total vesicle-vesicle interaction energy $E$ at any value of $\theta$ includes a negative (favorable) adhesion energy term and a positive (unfavorable) elastic stretching term (*5*, *6*, *14*)

$$E = 4\pi R^2 \left\{ K f^2(\theta) - \frac{W(1 - \cos\theta)[1 + f(\theta)]}{(3 - \cos\theta)} \right\} \quad (1)$$

where

$$f(\theta) = \frac{(3 - \cos\theta)}{2^{2/3}(1 + \cos\theta)^{1/3}(2 - \cos\theta)^{2/3}} - 1 \quad (2)$$

$W$ is the work of adhesion and $K$ is the elastic area expansion modulus of the membranes (*14*, *23*). The equilibrium condition (before water and solutes start flowing across the membrane to alleviate the stress) occurs when the energy $E$ is a minimum, at which point the contact angle $\theta = \theta_0$ and minimum energy $E = E_0$ are given by

$$W = 2K(1 - \cos\theta_0) f(\theta_0) \quad (3)$$

which gives

$$\cos\theta_0 \approx 1 - \left(\frac{2W}{K}\right)^{1/3} \quad (4)$$

and

$$E_0 = 4\pi R^2 W \left\{ \frac{f(\theta_0)}{2(1 - \cos\theta_0)} - \frac{(1 - \cos\theta_0)[1 + f(\theta_0)]}{(3 - \cos\theta_0)} \right\} \approx \frac{\pi^2 R^2 W^{4/3}}{4^{1/3} K^{1/3}} \quad (5)$$

Other relevant properties of two adhering vesicles interacting at constant internal (water) volume are equilibrium strain

$$\varepsilon_0 = \frac{\text{surface area increase}}{\text{original area}} = \frac{W}{2K(1 - \cos\theta_0)} = f(\theta_0) \quad (6a)$$

$$\approx \left\{\frac{W}{4K}\right\}^{2/3} \quad (6b)$$

equilibrium stress

$$\sigma_0 = K\varepsilon_0 = Kf(\theta_0) \approx (\tfrac{1}{4}WK^{1/2})^{2/3} \quad (7)$$

and intervesicle adhesion force

$$F_0 = 2\pi RW \quad (8)$$

All of the above values depend on only three properties: $R$, $W$, and $K$. A typical high value for $W$ is about 1 mJ $m^{-2}$, which has been measured for van der Waals and stress-enhanced hydrophobic contacts between uncharged lipid bilayers (*6*, *7*) and calcium-mediated binding interactions between charged lipid bilayers (*24*). A typical value for $K$ is ~100 mJ $m^{-2}$, which has been measured for both lipid bilayers and biological membranes (*14*). Putting these values into the above equations gives $\theta_0 = 45°$, $\varepsilon_0 = 0.02$ (2%), and $\sigma_0 = 2$ mN $m^{-1}$. Thus, once the interfacial energy exceeds about 1 mJ $m^{-2}$, the total surface area of each vesicle will be stretched by more than 2% of its initial (unstressed) area upon adhering. Because most lipid bilayers and biological membranes cannot be suddenly stretched beyond 2 to 4% without rupturing (*14*), one may conclude that an adhesion energy $W$ of about 1 mJ $m^{-2}$ is the highest that can be sustained without causing rupture and that large destabilizing stresses could already occur at lower adhesion energies.

Equations 5 and 8 show that intervesicle adhesion force and energy also depend on the radii, $R$, of the vesicles. For vesicle radii in the range of 10 to 100 nm, the above stresses and strains correspond to adhesion forces between $F_0 = 60$ and 600 pN and to adhesion energies in the range of $E_0 = 1.2 \times 10^{-19}$ to $120 \times 10^{-19}$ J (30 to 3000 $k_BT$, where $k_B$ is Boltzmann's constant and $T$ is temperature), respectively. These values are upper limits for the adhesion force and energy that can be attained with nonspecific surface forces.

Turning now to consider vesicle association through site-specific ligand-receptor

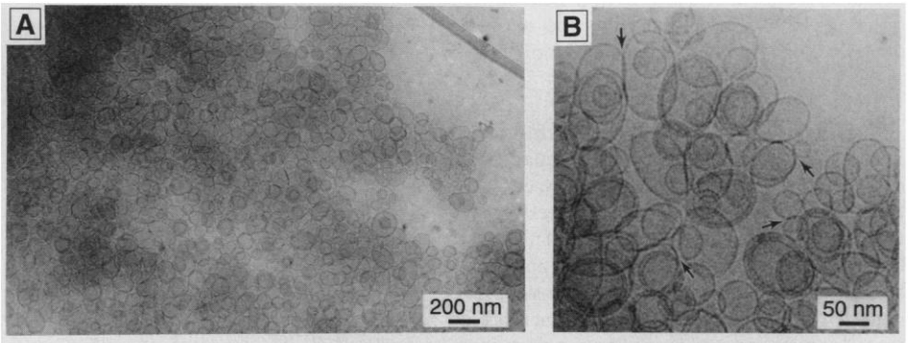


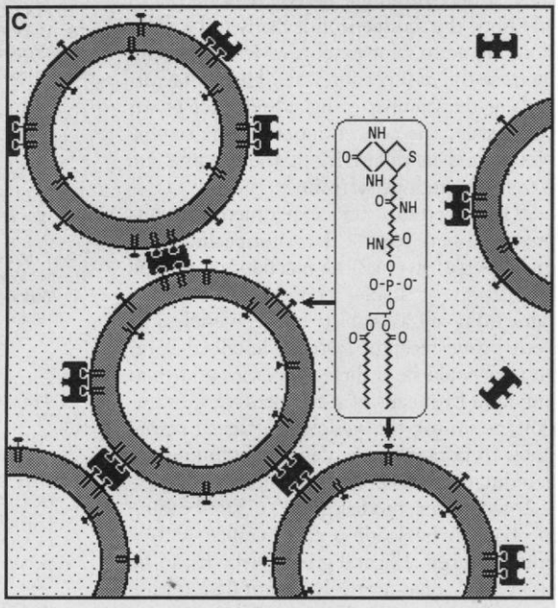


**Fig. 2.** (**A**) Low-resolution cryoelectron micrograph of multimicrometer-sized structure of DLPC vesicles containing DPPE-biotin after they were induced to aggregate by the addition of streptavidin to the solution. Before aggregation, the dispersed vesicles looked like those in Fig. 1A. (**B**) High-resolution cryoelectron micrograph of vesicle-vesicle contacts in the aggregate structure shown in (A). The individual vesicles are still spheroidal and minimally stressed. Arrows point to the contacts induced by the biotin-streptavidin coupling. (**C**) Schematic illustration of the geometry of the aggregated (tethered) vesicles of (A), which is quite different from the geometry of vesicles aggregated by nonspecific surface forces (Fig. 1). (**Inset**) DPPE-biotin molecule, which links to the soluble streptavidin molecule. Both DPPE-biotin and streptavidin were purchased from Molecular Probes (Eugene, Oregon).

binding, in the case of the well-studied biotin-avidin and analogous biotin-streptavidin systems (*21, 22, 25, 26*), the binding energies $E_0$ and adhesion forces $F_0$ per ligand-receptor bond have been measured only for certain combinations. These are $E_0$ = 30 to 35 $k_BT$ for soluble biotin with avidin, which corresponds to a binding constant of $K_a = e^{E_0/k_BT} = 10^{13}$ to $10^{15}$ (*21, 25*); $E_0$ = 15 to 16 $k_BT$ ($K_a = 10^6$ to $10^7$) for lipid-conjugated biotin with streptavidin (*18*); $F_0$ = 170 pN for lipid-conjugated biotin with avidin (*27*); and $F_0$ = 120 pN for lipid-conjugated desthiobiotin with avidin (*27*). Assuming that avidin and streptavidin bind in the same way, and defining the "effective" ligand-receptor bond length δ as

$$F_0\delta = E_0 \quad (9)$$

we obtain a value of $\delta \approx 15.5\ k_BT/170$ pN ≈ 0.37 nm for the effective bond length of lipid-conjugated biotin with streptavidin. Assuming a similar effective bond length for soluble biotin with streptavidin and applying this value to the binding energy, $E_0$ = 30 to 35 $k_BT$, of soluble biotin (for which $F_0$ is unknown) gives $F_0 \approx 400$ pN, whereas applying this value to the adhesion force of lipid-conjugated desthiobiotin (for which $E_0$ is unknown) gives $E_0 \approx 11\ k_BT$ ($K_a \approx 10^4$ to $10^5$). All of these values are reasonable and show that even one ligand-receptor bond between two small vesicles is already comparable to the strongest binding force attainable with nonspecific colloidal forces. Other potential advantages of site-specific binding mechanisms are (i) that very strong intervesicle binding should be achievable without deforming or stressing the membranes beyond the binding sites and (ii) that the whole process is highly controllable (by means of the concentrations of ligands and receptors on the surfaces) and reversible.

A rough estimate of the redispersion time can be made on the basis of the supposition that these times are limited by the lifetime of the biotin-streptavidin bond. In general, the characteristic lifetime of a ligand-receptor bond, τ, is given by the approximate general equation (*5*)

$$\tau \approx \tau_o\ e^{E_o/k_BT} \approx K_a\ \tau_o \quad (10)$$

where $\tau_o$ is the characteristic vibrational correlation time of the biotin group inside the avidin pocket, which is estimated to be on the order of $10^{-8}$ s (*28*). Inserting the above quoted values for lipid-conjugated biotin ($K_a = 10^6$ to $10^7$) and desthiobiotin ($K_a = 10^4$ to $10^5$) into Eq. 10 yields lifetimes of ~0.1 s and ~1 ms, respectively, for the two biotin-lipid homologues studied. These values may be compared with the measured redispersion times of ~1000 and ~100 s, respectively, which are much longer than the calculated bond lifetimes. However, given that multiple bonds must be broken to detach each vesicle and to break up the aggregated structures, these longer times are indeed reasonable. In addition, the redispersion is likely to be diffusion limited to some extent, which would also increase the redispersion time. Hence, factors such as the number of ligand-receptor bonds per vesicle, the concentration of the soluble biotin, and its diffusivity to the binding site govern the redispersion times.

The theoretical and experimental results presented here suggest that site-specific binding provides a practical mechanism for the production of stable secondary microstructures from self-assembled bilayer vesicles. In both ligand-receptor systems described here, vesicles could be tethered together and then unbound by means of a competitive substitution, returning the vesicles to their original state. In principle, one can predetermine the coordination number or stoichiometry of vesicle structures produced by a site-binding mechanism by loading each vesicle with a finite number of ligand groups, which can be easily and quantitatively controlled during vesicle preparation. The specificity of the binding can allow for even higher orders of self-assembly with multiple ligand-receptors and the sequential coupling of different vesicle populations of different sizes and compositions. The strength, controlled versatility, and reversibility offered by site-binding secondary self-assembly processes should enable the development of new classes of artificial biological structures and tissues and soft composite biomaterials with highly complex microstructures. Site-specific binding of vesicles and other membranes also offers the opportunity to perform specific and reversible flocculation of mixed colloidal systems, which may be valuable for advanced separations technology.

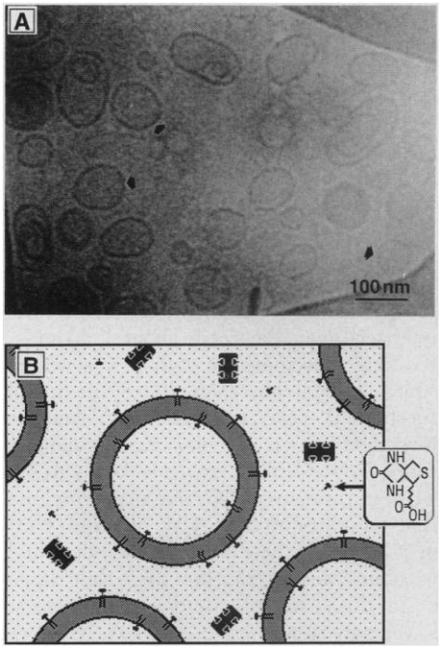


**Fig. 3.** (**A**) Redispersed vesicles from the aggregates of Fig. 2A after addition of soluble biotin. The soluble biotin binds much more strongly to the streptavidin than does the DPPE-biotin, leading to redispersion of the vesicle solution. Aggregation and redispersion could easily be monitored visually by observing the changing color of the solution between clear blue for dispersed vesicles to cloudy white for aggregated vesicles and back to clear blue for redispersed vesicles. Individual vesicles regained their spheroidal shapes and retained their original sizes. Compare to Fig. 1A. (**B**) Schematic of (A) showing inactivated streptavidin molecules in solution after the introduction of (**inset**) soluble biotin.

## REFERENCES AND NOTES


1. J. Israelachvili, in *Surfactants in Solutions*, K. L. Mittal and P. Bothorel, Eds. (Plenum, New York, 1986), vol. 4, pp. 3–33.
2. G. Cevc and D. Marsh, *Phospholipid Bilayers: Physical Principles and Models* (Wiley-Interscience, New York, 1985).
3. D. D. Lasic, *Liposomes from Physics to Applications* (Elsevier, Amsterdam, 1993).
4. J. H. Fendler, *Membrane Mimetic Chemistry* (Wiley, New York, 1982).
5. J. N. Israelachvili, *Intermolecular and Surface Forces* (Academic Press, London, 1992).
6. S. M. Bailey, S. Chiruvolu, J. N. Israelachvili, J. A. N. Zasadzinski, *Langmuir* **6**, 1326 (1990).
7. C. A. Helm, J. N. Israelachvili, P. M. McGuiggan, *Biochemistry* **31**, 1794 (1992).
8. M. Gratzl and G. Dahl, *FEBS Lett.* **62**, 142 (1976).
9. S. W. Hui, S. Nir, T. P. Stewart, L. T. Boni, S. K. Huang, *Biochim. Biophys. Acta* **941**, 130 (1988).
10. A. E. Sowers, Ed., *Cell Fusion* (Plenum, New York, 1987).
11. L. V. Chernomordik, G. B. Melikyan, Y. A. Chizmadzhev, *Biochim. Biophys. Acta* **906**, 309 (1987).
12. J. M. White, *Science* **258**, 917 (1992).
13. D. Papahadjopoulos, S. Nir, N. Düzgünes, *J. Bioenerg. Biomembr.* **22**, 157 (1990).
14. E. A. Evans and D. Needham, *J. Phys. Chem.* **91**, 4219 (1987).
15. L. D. Mayer, M. J. Hope, P. R. Cullins, *Biochim. Biophys. Acta* **858**, 161 (1986).
16. H. C. Loughrey, K. F. Wong, L. S. Choi, P. R. Cullis, M. B. Bally, *ibid.* **1028**, 73 (1990).
17. K.-D. Lee *et al. Biophys. J.* **64**, 905 (1993).
18. D. D. Powers, B. L. Willard, R. G. Carbonell, P. K. Kilpatrick, *Biotechnol. Prog.* **8**, 436 (1992).
19. K. Hashimoto, J. E. Loader, S. C. Kinsky, *Biochim. Biophys. Acta* **856**, 556 (1986).
20. J. R. Bellare, H. T. Davis, L. E. Scriven, Y. Talmon, *J. Electron Microsc. Tech.* **10**, 87 (1988).
21. N. M. Green, *Adv. Protein Chem.* **29**, 85 (1975).
22. W. Müller *et al.*, *Science* **262**, 1706 (1993).
23. R. M. Servuss and W. Helfrich, in *Physics of Complex and Supramolecular Fluids*, S. A. Safran and N. A. Clark, Eds. (Wiley, New York, 1987), pp. 85–100.
24. J. Marra, *Biophys. J.* **50**, 815 (1986).
25. M. Wilchek and E. A. Bayer, Eds., *Avidin-Biotin Technology* (Academic Press, San Diego, CA, 1990).
26. R. Blankenburg, P. Meller, H. Ringsdorf, C. Salesse, *Biochemistry* **28**, 8214 (1989).
27. E.-L. Florin, V. T. Moy, H. E. Gaub, *Science* **264**, 415 (1994).
28. W. C. Wimley and T. E. Thompson, *Biochemistry* **29**, 1296 (1990); H. Wennerström and B. Lindman, *Phys. Rep.* **52**, 1 (1979).


29. We thank W. Müller and H. Ringsdorf for supplying DODA-desthiobiotin and H. Gaub for a preprint of (*23*) and for helpful discussions on the strength of biotin-avidin bonds. Portions of this work were supported by National Institutes of Health grant GM47334 and National Science Foundation Materials Research Laboratory grant DMR-9123048.

9 February 1994; accepted 4 May 1994